Engineering 4 (2018) 881–887

Contents lists available at ScienceDirect

Engineering

journal homepage: www.elsevier.com/locate/eng

Research
Synthetic Biology—Article

A method for Absolute Protein Expression Quantity Measurement Employing Insulator RiboJ

Hongbin Yu [a,#], Zheng Wang [a,c,#], Hanyue Xu [a], Jiusi Guo [a,c], Qingge Ma [a,c], Xiangxu Mu [a,d], Yunzi Luo [a,b,*]

[a] West China Medical Center Team for International Genetically Engineered Machine Competition 2017, West China School of Medicine / West China Hospital, Sichuan University, Chengdu 610041, China
[b] Department of Gastroenterology, West China Hospital, Sichuan University and Collaborative Innovation Center of Biotherapy, Chengdu 610041, China
[c] West China School of Stomatology, West China Hospital, Sichuan University, Chengdu 610041, China
[d] College of Physical Science and Technology, Sichuan University, Chengdu 610064, China

ARTICLE INFO

Article history:
Received 7 March 2018
Revised 20 April 2018
Accepted 29 September 2018
Available online 09 October 2018

Keywords:
RiboJ
Promoter measurement
Synthetic biology

ABSTRACT

Measuring the absolute protein expression quantity for a specific promoter is necessary in the fields of both molecular biology and synthetic biology. The strength of a promoter is traditionally characterized by measuring the fluorescent intensity of the fluorescent protein downstream of the promoter. Until now, measurement of the absolute protein expression quantity for a promoter, however, has been unsuccessful in synthetic biology. The fact that the protein coding sequence influences the expression level for different proteins, and the inconvenience of measuring the absolute protein expression level, present a challenge to absolute quantitative measurement. Here, we introduce a new method that combines the insulator RiboJ with the standard fluorescence curve in order to measure the absolute protein expression quantity quickly; this method has been validated by modeling verification. Using this method, we successfully measured nine constitutive promoters in the Anderson promoter family. Our method provides data with higher accuracy for pathway design and is a straightforward way to standardize the strength of different promoters.

1. Introduction

As shown in the enzyme kinetic equations, enzyme concentration plays an important role, as well as substrate concentration, in enzymatic reactions. In order to enhance the efficiency of an artificial metabolic pathway with a predictable substrate concentration, the expression of each enzyme in this pathway should be carefully considered. Overproduction of an enzyme may cause an excessive burden for the cell. On the other hand, insufficient protein expression can result in low efficiency of the metabolic flux. Thus, the promoter, which influences the absolute protein expression quantity of the enzyme, should be chosen appropriately. However, a method of measuring the absolute protein expression quantity of a specific promoter has not yet been reported. The characterization of a promoter is traditionally performed by measuring the fluorescent intensity or RT-PCR results [1–6] of the downstream protein or gene, which can only be compared in a relative manner. However, certain challenges affect the measurement of the absolute protein expression quantity of a specific promoter. The dynamics of gene expression are influenced by the protein coding sequences; this means that measuring a promoter by simply detecting its downstream protein expression level is not accurate [7]. In addition, it is inconvenient and expensive to measure the absolute protein expression quantity using western blotting, ELISA, or similar techniques.

RiboJ is a ribozyme that self cleaves, thereby removing the upstream region and, most importantly, the 5′ untranslated region. In the work of Lou et al. [7], the relative expression levels of two different variants of green fluorescence protein (GFP) (i.e., sfGFP and cl-sfGFP fusion) were not the same. However, when they added RiboJ before the coding region, the relative expression levels for the induction curves collapsed. This finding indicated that RiboJ can act as an insulator to homogenize the relative protein expression level for a given promoter, thereby making it possible to evaluate the protein expression ability of a specific promoter on a large scale, regardless of the coding sequence. To characterize

* Corresponding author.
E-mail address: luoyunzi@scu.edu.cn (Y. Luo).
# These authors contributed equally to this work.

https://doi.org/10.1016/j.eng.2018.09.012

the promoter in a quick and simple way, we attempted to determine the relationship between absolute protein quantity and enhanced green fluorescence protein (eGFP) fluorescence by making an eGFP fluorescence standard curve, and then using a protein expression system with a RiboJ design to determine the promoter strength. We chose nine promoters from the Anderson promoter family, which is an σ70 transcriptional promoter library of *Escherichia coli* (*E. coli*). The Anderson promoter family is widely used in the International Genetically Engineered Machine (iGEM) Competition, and has been characterized by expressing red fluorescence protein (RFP) and GFP [4,8]. Our design allowed us to successfully measure these nine promoters, and yielded higher-accuracy data for future pathway design. Our method also provides a straightforward way to standardize the strength of different promoters. Thus, this paper introduces a novel method to measure the absolute protein expression quantity of any constitutive promoter.

2. Materials and methods

2.1. Plasmids construction

The pET28a-eGFP plasmid was obtained from the State Key Laboratory of Biotherapy, in China. The eGFP gene was originally obtained from plasmid pEGFP-N1, and was then ligated into pET28a vector with a 6×His tag for purification. The measurement plasmid originated from BBa_J364001 in the pSB1C3 vector from the Registry of Standard Biological Parts. RiboJ was generated from synthetic oligos (TsingKe Biological Technology Co., Ltd., China) and was seamlessly added to the downstream of Anderson promoter sequence by means of Gibson assembly. The GFP was then replaced by eGFP by means of Gibson assembly in order to construct the final measurement device with a J23106 promoter. The other measurement devices, with different promoters, were generated by oligonucleotide-directed mutagenesis (KOD-Plus-Neo, TOYOBO Co., Ltd., Japan; DpnI, New England Biolabs Inc., USA). The sequences for the Anderson promoters are documented in the Registry of Standard Biological Parts [8]. The plasmids used in the study are listed in Table 1. The gene structure of the measurement device is shown in Fig. 1, and the sequence is documented in the Appendix A (Table S1).

2.2. Purification of the eGFP

The expressing plasmid (pET28a-eGFP) was transformed into *E. coli* BL21(DE3) cells. Transformed cells were grown in 1 L lysogeny broth (LB) supplemented with 34 $\mu g \cdot mL^{-1}$ kanamycin at 37 °C, with agitation at 220 $r \cdot min^{-1}$ overnight. When the OD_{600} (optical density measured at a wavelength of 600 nm) reached 0.6–0.8, the cells were induced with a final concentration of 0.5 $mmol \cdot L^{-1}$ isopropyl β-*D*-1-thiogalactopyranoside (IPTG). After being cultured for a further 18 h at 16 °C, the cells were harvested by centrifugation at 4 °C and 4000 $r \cdot min^{-1}$ for 10 min. The harvested cells were suspended in 40 mL lysis buffer (PBS buffer, 140 $mmol \cdot L^{-1}$ NaCl, 2.7 $mmol \cdot L^{-1}$ KCl, 10 $mmol \cdot L^{-1}$ Na_2HPO_4, and 1.8 $mmol \cdot L^{-1}$ KH_2PO_4, at pH 7.5) and lysed by a high-pressure homogenization instrument (JN-02C, JNBIO Co., Ltd., China). The lysate was then subjected to centrifugation (4 °C, 15 000 $r \cdot min^{-1}$, 30 min; Thermo F21-8x50y rotor). The clear supernatant was collected and loaded onto a nickel-nitrilotriacetic acid (Ni-NTA) column pre-equilibrated with the lysis buffer at 4 °C, and the pellets were discarded. The column was washed three times with 3–5 column volume (CV) of washing buffer (10 $mmol \cdot L^{-1}$ imidazole dissolved in PBS buffer) and three times with 3–5 CV of elution buffer (200 $mmol \cdot L^{-1}$ imidazole dissolved in PBS buffer). The eluted protein containing eGFP was concentrated in a 15 mL concentrator (Amicon® Ultra-15, Merk Millipore, USA) before being loaded onto the Superdex 75 10/300 GL (GE Healthcare Conglomerate, USA). The single peak of eGFP was collected, and the eGFP was concentrated to 25 $mg \cdot mL^{-1}$. Part of the protein was analyzed immediately; the remaining portion was frozen using liquid nitrogen and kept in stock at −80 °C. We repeated the purification method five times and obtained five batches of purified eGFP for further measurement.

Table 1
Plasmids used in this study.

Plasmid name	Description
pJ23100	Measurement device containing promoter J23100
pJ23106	Measurement device containing promoter J23106
pJ23107	Measurement device containing promoter J23107
pJ23108	Measurement device containing promoter J23108
pJ23109	Measurement device containing promoter J23109
pJ23113	Measurement device containing promoter J23113
pJ23114	Measurement device containing promoter J23114
pJ23117	Measurement device containing promoter J23117
pET28a-eGFP	eGFP gene inserted into a pET28a plasmid for protein purification

2.3. eGFP stability test

We measured the fluorescence intensity of each batch of eGFP immediately after purification in order to exclude the impact of fluorescence quenching. The eGFP sample was placed in a black 96-well plate fully covered with aluminum foil before measuring, and was then measured by means of a Spark™ 10 M (Tecan Group Ltd., Switzerland) provided by the West China School of Pharmacy at Sichuan University. The fluorescence intensity was measured with an excitation wavelength of 450 nm and an emission wavelength of 490 nm. The absolute protein concentration of the purified eGFP was measured using BCA Protein Assay Kit (Sangon Biotech (Shanghai) Co., Ltd., China). The experiment was repeated five times to test its repeatability.

The first batch of purified eGFP was stored at −80 °C; we then repeatedly measured the fluorescence intensity and absolute protein concentration 4, 8, 12, and 16 d after purification in order to test the stability of the eGFP and identify the impact of fluorescence quenching over time for our experiment.

2.4. Cell density and fluorescence measurement

Our measurement process followed the routine of the iGEM InterLab study to a large extent [9]. All the measurement devices were transformed into *E. coli* BL21 (DE3). Transformed cells were grown overnight at 37 °C and 220 $r \cdot min^{-1}$, in 5 mL LB medium with 25 $\mu g \cdot mL^{-1}$ chloramphenicol. At least three colonies per device were picked on the plate for measurement. The cultures were diluted to a target OD_{600} of 0.02 in 12 mL LB medium with 25 $\mu g \cdot mL^{-1}$ chloramphenicol in a 50 mL falcon tube, and incubated

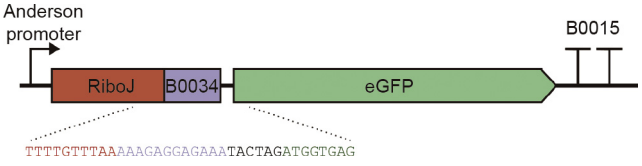

Fig. 1. Gene structure of the measurement device. The diagram above portrays the measurement device gene structure, in which there is no sequence between the Anderson promoter and the insulator RiboJ. Part of the gene sequence is shown below, colored to align with the elements above. B0034 is a ribosome binding site and B0015 is a double terminator; their description and sequence are documented in the Registry of Standard Biological Parts.

at 37 °C and 220 r·min^{-1}. Three replicates, with 500 μL of LB medium each, were sampled from each tube for measurement after being incubated overnight (16–18 h). Cell density (OD) was measured at a wavelength of 600 nm, and the fluorescence intensity of the bacteria was measured with an excitation wavelength of 450 nm and an emission wavelength of 490 nm (Spark™ 10 M, Tecan Group Ltd., Switzerland).

2.5. Modeling and data analysis

This section first discusses the theory of protein production relative to promoter activity [10,11]. The velocity of the production per cell of eGFP mRNA molecules (M_{eGFP}) is relative to the copy number (n), promoter activity (PoPs), and mRNA degradation rate ($\gamma_{M_{eGFP}}$), as described in Eq. (1). The amount of immature eGFP per cell (I_{eGFP}) is dependent on the immature eGFP translation rate (k_{tr}^{eGFP}), mature eGFP degradation rate ($\gamma_{I_{eGFP}}$), and mature eGFP translation rate (k_{m}^{eGFP}), as shown in Eq. (2). The amount of mature eGFP per cell (P_{eGFP}) is also affected by the degradation rate of mature eGFP ($\gamma_{P_{eGFP}}$), as shown in Eq. (3).

$$\frac{dM_{eGFP}}{dt} = n\text{PoPs} - \gamma_{M_{eGFP}} M_{eGFP} \quad (1)$$

$$\frac{dI_{eGFP}}{dt} = k_{tr}^{eGFP} M_{eGFP} - \gamma_{I_{eGFP}} I_{eGFP} - k_{m}^{eGFP} I_{eGFP} \quad (2)$$

$$\frac{dP_{eGFP}}{dt} = k_{m}^{eGFP} I_{eGFP} - \gamma_{P_{eGFP}} P_{eGFP} \quad (3)$$

The equation system can be solved with Mathematica (Wolfram Research, USA):

$$P_{eGFP} = f\left(n,\ \gamma_{M_{eGFP}},\ k_{tr}^{eGFP},\ \gamma_{I_{eGFP}},\ k_{m}^{eGFP},\ \gamma_{P_{eGFP}},\ t\right) \times \text{PoPs} \quad (4)$$

where f is a function of the $\gamma_{M_{eGFP}}$, $\gamma_{I_{eGFP}}$, $\gamma_{P_{eGFP}}$, k_{tr}^{eGFP}, k_{m}^{eGFP}, n, and t. For one type of promoter, we regard $\gamma_{M_{eGFP}}$, $\gamma_{I_{eGFP}}$ and so on as a constant, referred to as A. Next, after analyzing the data of fluorescence from the fluorescence experiments using linear regression, the coefficient (k) between concentration of (C_{eGFP}) and fluorescence intensity (F) can be obtained.

$$C_{eGFP} = kF \quad (5)$$

Finally, we performed a series of experiments to obtain the relationship between the fluorescence and the concentration, and thus created a scale for the promoters. The molarity of the eGFP (M_{reCFP}) can be written as follows, and it was found to be 31 534.35 Da:

$$C_{meGFP} = \frac{C_{eGFP}}{M_{reCFP}} \quad (6)$$

$$C_{cell} = \text{OD}/\varepsilon \quad (7)$$

where C_{meGFP} is the concentration of 1 mol eGFP, C_{cell} is the concentration of cells, and ε is a constant with a value of 8×10^8 [12]. Thus, the promoter activity A can be written as follows:

$$A = \frac{k\varepsilon F}{M_{reCFP}\text{OD}} \quad (8)$$

N colonies were picked. We measured the fluorescence intensity and cell density M times for each colony and then measured the fluorescence intensity and OD Q times for the control (LB medium). The equation can be written as follows:

$$A = \frac{k\varepsilon}{M_{eCFP}} \times \frac{1}{N} \sum_{n=1}^{N} \frac{\frac{1}{M}\sum_{m=1}^{M} F_{nm} - \frac{1}{Q}\sum_{q=1}^{Q} F_{nq}^{LB}}{\frac{1}{M}\sum_{m=1}^{M} \text{OD}_{nm} - \frac{1}{Q}\sum_{q=1}^{Q} \text{OD}_{nq}^{LB}} \quad (9)$$

3. Results

3.1. eGFP purification results

We were able to successfully obtain the purified eGFP. The gel filtration result showed a single peak in the sample (Fig. 2(a)). Samples analyzed by sodium dodecyl sulfate–polyacrylamide gel electrophoresis (SDS-PAGE) revealed an about 30 kDa induction band (Fig. 2(b)). The size of this band was consistent with the predicted mass of the recombinant enzyme.

3.2. eGFP stability test

We analyzed by linear regression the results of five independent experiments in which the eGFP was freshly purified. Our findings indicated a strong linear correlation between the fluorescence intensity and the absolute protein concentration (C) measured by BCA assays in our experiment range (r^2 = 0.9733, Fig. 3). The results show that the experiment possesses excellent repeatability.

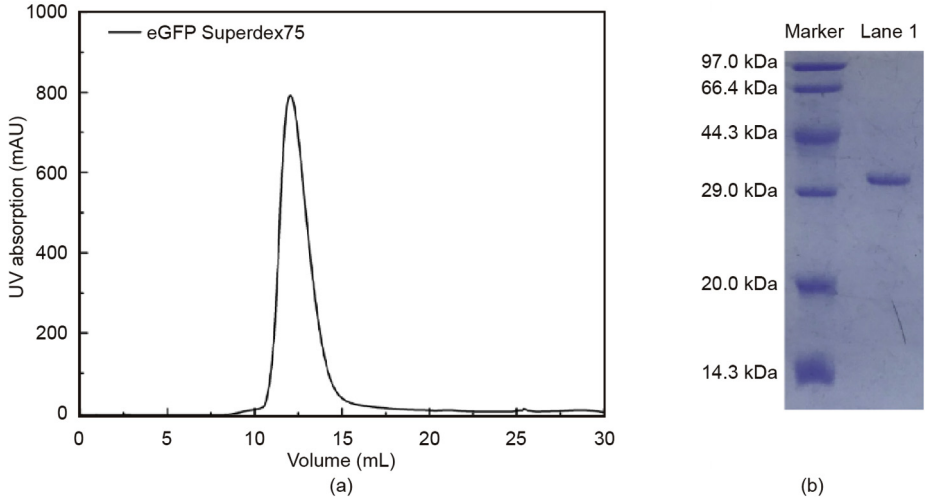

Fig. 2. (a) Gel filtration purification of eGFP; (b) SDS-PAGE result of the purified eGFP (31.5 kDa) in Lane 1. The protein was obtained from *E. coli* BL21(DE3) transformed with pET28a-eGFP.

Next, we collected all the data from the fluorescent quenching experiment, as shown in Fig. 4. The data collected by continuous measurement over 16 d was analyzed by linear regression. The results showed that the fluorescence intensity of the eGFP and the absolute protein concentration show a strong linear correlation (r^2 = 0.9936); this means that the purified eGFP has a level of high stability and can resist quenching over time, because the measurement results from each time were similar and formed a linear correlation.

3.3. Data analysis

After measuring the OD_{600} and fluorescence intensity for the measurement device using the method described above, the data were collected and the results were calculated. The original measurement results are documented in the Appendix A (Tables S2 and S3). The absolute protein expression quantity and relative activity of the promoters are shown in Table 2 and Fig. 5.

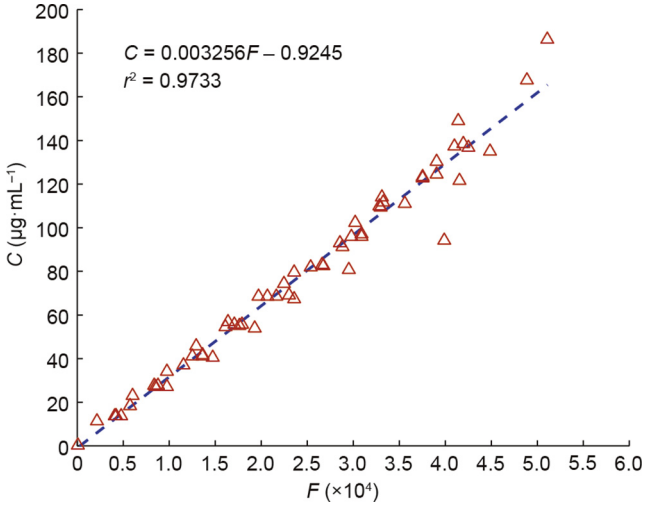

Fig. 3. The fluorescence intensity and absolute protein concentration have a linear correlation for the eGFP measured at 450/490 nm. This figure includes data from five independent experiments, which exhibit excellent linear correlation, thus indicating that the experiment possesses excellent repeatability.

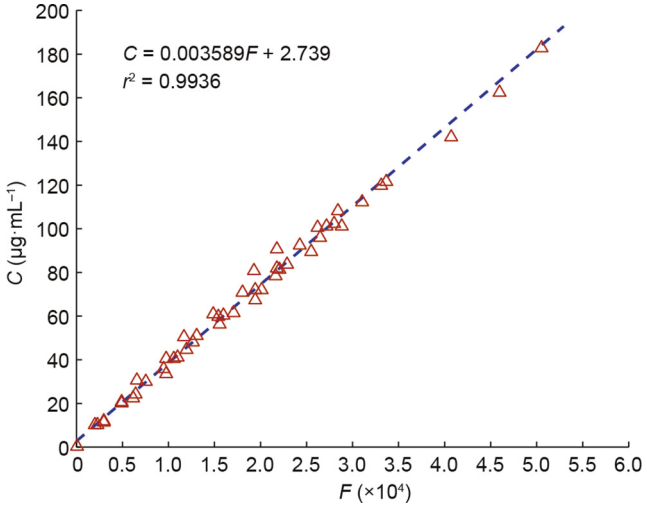

Fig. 4. The fluorescence intensity and absolute protein concentration have a linear correlation for the eGFP measured at 450/490 nm. This figure includes all the data from the continuous detection experiment, which shows a strong linear correlation.

Table 2
Absolute protein expression quantity and promoter relative activity of the measured promoters.

Promoter	Absolute protein expression quantity (μmol·mL^{-1})	Relative activity
J23100[a]	1.893 ± 0.070	1.000
J23106	1.344 ± 0.062	0.710
J23107	0.464 ± 0.011	0.244
J23108	0.875 ± 0.138	0.462
J23109	0.237 ± 0.010	0.125
J23113	0.227 ± 0.009	0.120
J23114	0.200 ± 0.006	0.106
J23117	0.160 ± 0.005	0.085

[a] The J23100 result was set at 1 for relative activity comparison.

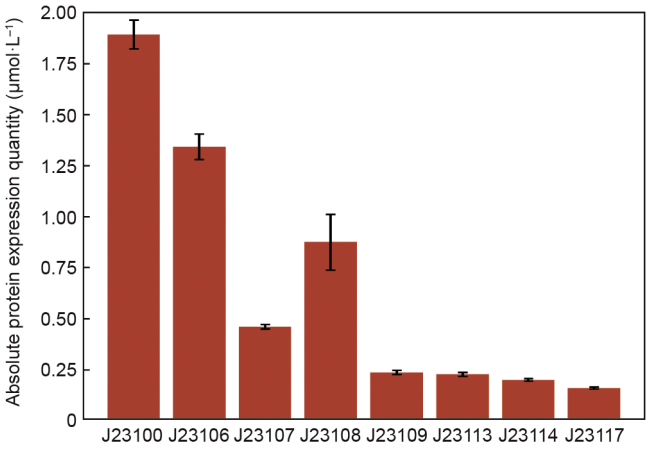

Fig. 5. Absolute protein expression quantity of the measured promoters.

It is notable that the time-invariance character of the promoter can be demonstrated by the modeling data. According to Table 2, Eq. (4), and the experimental results, the rate of protein production can be determined, as shown in Fig. 6. The proportion of accumulated protein expressed by different promoters over different times is the same. Fig. 6(b–d) show the protein expression proportion based on the experimental result at a given time.

4. Discussion

Absolute protein expression quantity is important for quantitative pathway construction, which has rarely been reported to date. The quantitative measurement of promoter activity that was attained in this study is useful in promoter selection. To verify the usefulness of our method, we selected a three-enzyme metabolic pathway as an example.

We set $[E_t]$ as the total concentration of the enzyme, $[E]$ as enzyme concentration, $[S]$ as the substrate concentration, $[ES]$ as the concentration of the enzyme-substrate complex, $[P]$ as the product concentration, k_1 as the equilibrium constant of the first positive reaction, k_2 as the equilibrium constant of the first reverse reaction, and k_3 as the equilibrium constant of the second positive reaction [13].

The chemical equation can be written as follows:

$$[E] + [S] \underset{k_2}{\overset{k_1}{\rightleftharpoons}} [ES] \xrightarrow{k_3} [E] + [P] \tag{10}$$

Assuming that each part of the reaction has reached equilibrium, the production and degradation rates of $[ES]$ are equal.

$$k_1([E_t] - [ES])[S] = k_2[ES] + k_3[ES] \tag{11}$$

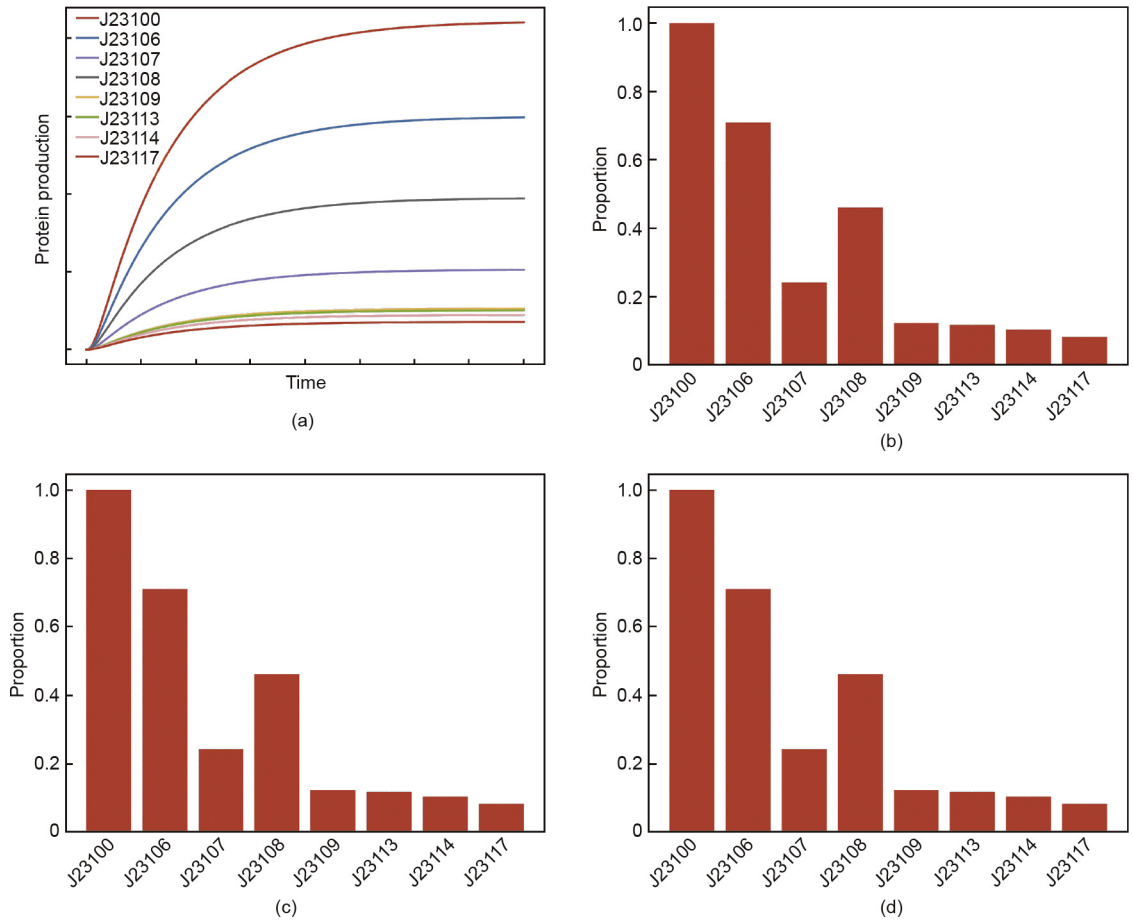

Fig. 6. (a) The modeling result of the time-invariance character of the promoters; (b) the proportion of protein expressed by the promoters after a quarter of the process is complete; (c) the proportion of protein expressed by the promoters after half of the process is complete; (d) the proportion of protein expressed by the promoters at the end of the process. The height of each bar in parts (b–d) represents the proportion of the protein expressed by each promoter to the protein expressed by J23100.

Rearranging this equation gives the following:

$$\frac{([E_t]-[ES])[S]}{[ES]}=\frac{k_2+k_3}{k_1} \tag{12}$$

Assuming that

$$K_M=\frac{k_2+k_3}{k_1} \tag{13}$$

$$v=k_3[ES] \tag{14}$$

Eq. (12) become the following:

$$[ES]=\frac{[E_t][S]}{K_M+[S]} \tag{15}$$

$$v=\frac{k_3[S]}{K_M+[S]}[E_t] \tag{16}$$

Note that the reaction of $[P]$ and $[E]$ was ignored, even though $[P]$ will influence the equilibrium, which will affect the production rate. Therefore, as time passes, Eq. (16) may become less accurate. Nevertheless, generally speaking, it is able to describe this process.

Assuming the pathway through which compound A becomes C includes two reactions with two enzymes required, P_1 and P_2:

$$a\mathrm{A}\xrightarrow{P_1}b\mathrm{B} \tag{17}$$

$$c\mathrm{B}\xrightarrow{P_2}d\mathrm{C} \tag{18}$$

The reaction rates of these two reactions are represented by v_1 and v_2, and the concentrations of compound A, B, and C are $[A]$, $[B]$, and $[C]$.

Without considering spontaneous degradation, the net reaction rate of one compound (A, B, or C) is equal to its generation rate minus its consumption rate, assuming that the proportions of each reaction are 1:1.

$$\frac{\mathrm{d}[A]}{\mathrm{d}t}=-v_1 \tag{19}$$

$$\frac{\mathrm{d}[B]}{\mathrm{d}t}=-v_2+\frac{b}{a}v_1 \tag{20}$$

$$\frac{\mathrm{d}[C]}{\mathrm{d}t}=\frac{d}{c}v_2 \tag{21}$$

Whether it is a first-order reaction or a zero-order reaction, the rate is only determined by the concentration of enzyme, when the type of enzyme and the initial concentration of the substrate are given (as shown in Eq. (16)). It is apparent that the higher the concentration of enzyme is, the faster the reaction will be. If there is a major difference between the enzyme's maximum rate, $V_{max}=k_{cat}[E_t]$, of two reactions, then the product of one of the reactions cannot be produced, which limits the metabolic rate. Therefore, there is a global best solution to optimize the reactions for multi-step enzyme catalysis (Fig. 7).

However, if V_{max} is adjusted, the product will not accumulate (Fig. 8). Therefore, appropriate promoters must be chosen in order

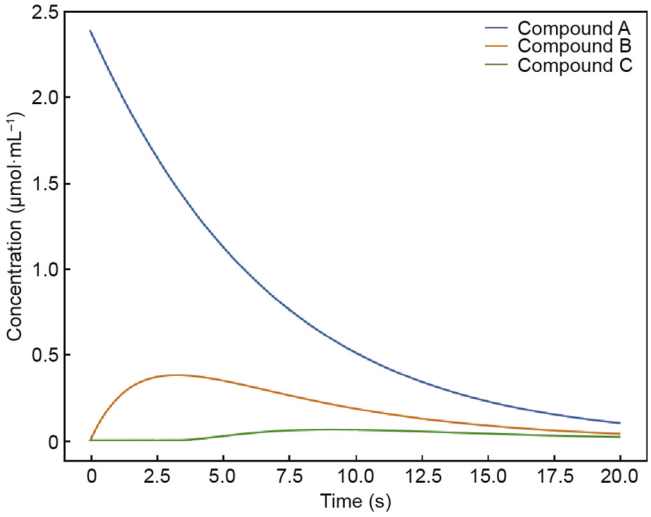

Fig. 7. The concentration variation of substrates. The V_{max} ratio of the three reactions is 1:5:29.

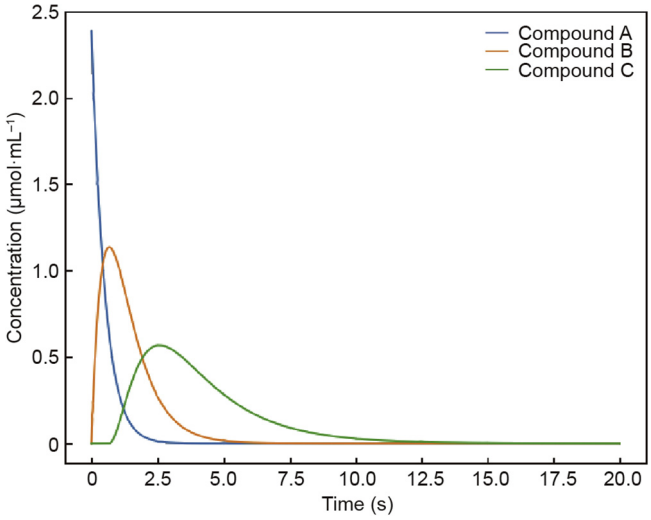

Fig. 8. The concentration variation of the substrates. The V_{max} ratio of the three reactions is 1:2:2.

to make V_{max} of each of the three reactions equal. The method described in this paper is an appropriate method of doing so. Given the promoter activity obtained earlier, it is possible to accurately calculate the concentration of protein (C_{eGFP}), which is equal to [E].

The modeling results indicate that [E] plays an important role in the metabolic pathway construction. Thus, we have introduced a novel and quick method for absolute protein expression quantitative measurement that will be useful in future applications. Furthermore, the promoter data and gene structure provided by our method can be used directly for metabolic pathway construction in the future.

In addition, we have provided a straightforward way to standardize the strength of different promoters, since the evaluation standard based on the absolute protein quantity can be used directly for all promoters. We have introduced this standardized method and the RiboJ design in order to encourage researchers to characterize promoters using universally comparable parameters (e.g., absolute protein quantity), and to employ the insulator RiboJ to promote the repeatability and transplantability of gene circuit design in different research studies. Furthermore, the ranking of the relative strength of promoters that was performed in this study differs from the ranking that is based on simple RFP fluorescence intensity measurement, as documented in the Registry of Standard Biological Parts [14]. The difference may be caused by the RiboJ design in our research, which can significantly influence the expression quantity [7,15]. Thus, our method provides greater accuracy in measurement results and gene structure, which will assist pathway construction in the future.

5. Conclusion

In this study, we introduced a novel method to measure the absolute protein expression quantity of a specific promoter. We then utilized our method to successfully measure nine constitutive promoters in the Anderson promoter family, and achieved results that differ from the fluorescent intensity measurement results reported in the literature. Our method provides data with greater accuracy, and offers a straightforward way to standardize the strength of different promoters.

Compliance with ethics guidelines

Hongbin Yu, Zheng Wang, Hanyue Xu, Jiusi Guo, Qingge Ma, Xiangxu Mu, and Yunzi Luo declare that they have no conflict of interest or financial conflicts to disclose.

Acknowledgements

This work was supported by Fundamental Research Funds for Central Universities to Yunzi Luo, the National Natural Science Foundation of China (81502966) and the China Innovation and Entrepreneurship Training Program for Undergraduates (201710611744). We are thankful for the support from our principal investigator (PI) and instructors: Prof. Yunzi Luo, our PI, who provided the lab and supervision necessary for us to finish this project, and Prof. Dan Su, who also provided a lab for us. We thank Huayi Liu and Liping Wang from Yunzi Luo's lab, and Yiping Chen from Dan Su's lab of the State Key Lab of Biotherapy for their advice. We also thank other team members from West China Medical Center of Sichuan University for iGEM 2017, and Wen Guo and Yifan Zhong especially. We thank the West China School of Medicine / West China Hospital and the State Key Lab of Biotherapy for their support. We thank the iGEM foundation for providing the opportunity for us to take part in the worldwide biology competition to start our research.

Appendix A. Supplementary data

Supplementary data to this article can be found online at https://doi.org/10.1016/j.eng.2018.09.012.

References

[1] Maeda M, Shimada T, Ishihama A. Strength and regulation of seven rRNA promoters in *Escherichia coli*. PLoS ONE 2015;10(12):e0144697.
[2] Rudge TJ, Brown JR, Federici F, Dalchau N, Phillips A, Ajioka JW, et al. Characterization of intrinsic properties of promoters. ACS Synth Biol 2016;5(1):89–98.
[3] Pedraza JM, Van Oudenaarden A. Noise propagation in gene networks. Science 2005;307(5717):1965–9.
[4] Chappell J, Freemont P. *In vivo* and *in vitro* characterization of σ^{70} constitutive promoters by real-time PCR and fluorescent measurements. In: Polizzi KM, Kontoravdi C, editors. Synthetic biology, 1073. Totowa: Humana Press; 2013. p. 61–74.
[5] Kelly JR, Rubin AJ, Davis JH, Ajo-Franklin CM, Cumbers J, Czar MJ, et al. Measuring the activity of BioBrick promoters using an *in vivo* reference standard. J Biol Eng 2009;3(1):4.
[6] Luo Y, Zhang L, Barton KW, Zhao H. Systematic identification of a panel of strong constitutive promoters from *Streptomyces albus*. ACS Synth Biol 2015;4(9):1001–10.

[7] Lou C, Stanton B, Chen Y, Munsky B, Voigt CA. Ribozyme-based insulator parts buffer synthetic circuits from genetic context. Nat Biotechnol 2012;30(11):1137–42.
[8] Anderson JC. Anderson promoter collection [Internet]. 2018 [cited 2018 Mar 6]. Available from: http://parts.igem.org/Promoters/Catalog/Anderson.
[9] Beal J, Haddock-Angelli T, Gershater M, De Mora K,Lizarazo M, Hollenhorst J, et al. Reproducibility of fluorescent expression from engineered biological constructs in *E. coli*. PLOS One 2016;11(3):e0150182.
[10] Song K. Introduction to synthetic biology. Beijing: Science Press; 2010. Chinese.
[11] Deft TU. Modeling [Internet]. 2018 [cited 2018 Mar 6]. Available from: http://2015.igem.org/Team:TU_Delft/Modeling.
[12] Agilent. *E. coli* cell culture concentration from OD_{600} calculator [Internet]. 2018 [cited 2018 Mar 6]. Available from: https://www.genomics.agilent.com/biocalculators/calcODBacterial.jsp.
[13] Berg JM, Tymoczko JL, Stryer L, editors. Biochemistry: a short course. New York: W. H. Freeman and Company; 2012.
[14] Anderson JC. Strength of Anderson Promoter [Internet]. 2018 [cited 2018 Mar 6]. Available from: http://parts.igem.org/wiki/index.php/Part:BBa_J23100.
[15] William and Mary Team. RiboJ [Internet]. 2018 [cited 2018 Apr 19]. Available from: http://2016.igem.org/Team:William_and_Mary/RiboJ.